Int J Clin Exp Pathol 2024;17(12):458-468
www.ijcep.com /ISSN:1936-2625/IJCEP0161189

Original Article

Bmi-1 plays an important role in preventing bone aging by regulating the bone microenvironment

Li Liu[1], Yuanqing Huang[2]

[1]*School of Nursing, Hunan University of Medicine, No. 492 Jinxi South Road, Huaihua 418000, Hunan, China;*
[2]*School of Stomatology, Hunan University of Medicine, No. 492 Jinxi South Road, Huaihua 418000, Hunan, China*

Received October 14, 2024; Accepted November 18, 2024; Epub December 15, 2024; Published December 30, 2024

Abstract: Background: B-cell specific Moloney MLV insertion site-1 (Bmi-1) belongs to the polycomb group (PcG) gene and is a transcriptional suppressor to maintain appropriate gene expression patterns during development. To investigate whether the Bmi-1 gene has a corrective effect on bone senescence induced in Bmi-1$^{-/-}$ mice through regulating the bone microenvironment. Methods: Littermate heterozygous male and female mice (Bmi-1$^{+/-}$) were used in this study. Related experiments were performed in wild type mice (10 mice, WT group) and Bmi-1 knock out mice (10 mice, BKO group) for analysis of phenotype, skeletal radiography, micro-computed tomography, histology, immunohistochemical staining, western blot analysis, and detection of ROS levels. Results: Our results indicated that the Bmi-1 gene could proportionally rescued mice suffering from bone aging induced by Bmi-1 gene defects. Bmi-1 plays an anti-aging effect in bone through multiple aspects, such as increasing osteoblast bone formation and decreascing osteoclast bone absorption, stimulating proliferation, reducing apoptosis, inhibiting reactive oxygen species (ROS) and delaying DNA damage. Conclusions: Our results suggested that Bmi-1 may play a fundamental and important role in correcting bone senescence in BKO mice. At the same time, it may provide theoretical basis for the clinical application of Bmi-1 in anti-aging in bone.

Keywords: Bmi-1, bone senescence, osteoblast, osteoclast, bone microenvironment

Introduction

Bone senescence, like osteoporosis, is a bone metabolic disease that results in degenerative skeletal disorder and increased risk of fracture [1, 2]. “Free Radical Theory of Aging” has established that reactive oxygen species (ROS) are produced endogenously from normal cellular metabolic processes [3]. In the theory, unbalance between antioxidants and ROS leads to the occurrence of oxidative stress that damages various macromolecules. There is substantial evidence to support that high production of ROS is strongly associated with age-related bone diseases.

B-cell specific Moloney MLV insertion site-1 (Bmi-1) belongs to the polycomb group (PcG) gene and is a transcriptional suppressor that maintains appropriate gene expression patterns during development [4]. Previous study confirmed that the Bmi-1 gene could regulate cell cycling and senescence by inhibiting the p16^{INK4a}/Rb and p19^{AFR}/p53 signal pathways [5]. Bmi-1 gene knockout mice (BKO) suffer from premature aging accompanied by serious defects in stem cell self-renewal and in maintaining normal mitochondrial physiological function [6, 7]. The accumulation of ROS caused by impaired mitochondrial function in Bmi-1 knockout mice leads to DNA damage. However, the changes are reversible with the addition of antioxidants such as n-acetyl-l-cysteine (NAC) or pyrroloquinoline quinone (PQQ) [8-10].

Previous studies have shown that PQQ can protect mitochondria from oxidative stress-induced DNA damage [11-14]. Further studies demonstrated that PQQ plays a role in scavenging oxygen free radicals during oxidative stress [15]. However, the mechanism underlying the effect of the Bmi-1 gene on bone senescence is still unclear.

https://doi.org/10.62347/DIIJ2884

To investigate the potential role of the Bmi-1 gene, in the study, we utilize BKO mice to induce typical premature aging and bone aging phenotypes. We speculate whether Bmi-1 gene plays an important role in anti-aging in bone by regulating the bone microenvironment.

Materials and methods

Mice and genotyping

Bmi-1 heterozygote (Bmi-1$^{+/-}$) mice (129Ola/FVB/N hybrid back-ground) were backcrossed 10-12 times to the C57BL/6J background and mated to generate the Bmi-1 knock out homozygote (Bmi-1$^{-/-}$, BKO) and their wild-type (WT) littermates genotyped by PCR [16, 17]. Mice were maintained in the Experimental Animal Center of Nanjing Medical University. All animal experiments were carried out in strict accordance with the Guidelines of the Institute for Laboratory Animal Research of Nanjing Medical University. The protocol was approved by the Committee on the Ethics of Animal Experiments of Nanjing Medical University.

Animal grouping

Mice were divided into 2 groups of 10 mice each and treated as following: WT group: 3-week weaning littermate wild type mice were fed normal diet for 4 weeks; and the BKO group: 3-week weaning littermate Bmi-1 knockout mice were fed normal diet for 4 weeks.

Seven weeks later, the 2 groups of 10 mice each were sacrificed for further studies. The 7-week-old mice were divided into two groups according to being either WT or BKO. After ethyl ether anesthesia, photos were taken, and the cervical vertebra was dislocated immediately. The tibia and femur were dissected and fixed with 75% alcohol.

Analysis of mouse phenotype, percent survival, and body weight

To investigate effect of Bmi-1 on phenotype, animals were divided into 2 groups of 10 mice each (WT group, BKO group). We carried out statistical analysis of phenotype, body weight, and percent survival with descriptive analysis, arithmetic mean, and survival time in two groups mice.

Skeletal radiography

Tibias and femurs were removed and dissected free of soft tissue. Contact radiographs were taken using a FaxitronModel 805 radiographic inspection system (Faxitron Contact, Faxitron, Germany; 22 kV and 4-minute exposure time). X-Omat TL film (Eastman Kodak Co., Rochester, NY, USA) was used and processed routinely.

Micro-computed tomography (μCT)

Tibias obtained from 7-week-old mice were dissected free of soft tissue, fixed overnight in 70% ethanol, and analyzed by μCT with a SkyScan 1072 scanner and associated analysis software (SkyScan, Antwerp, Belgium). Briefly, image acquisition was performed at 100 kV and 98 μA with a 0.9-degree rotation between frames. During scanning, the samples were enclosed in tightly fitting plastic wrap to prevent movement and dehydration. Thresholding was applied to the images to segment the bone from the background. Two dimensional images were used to generate 3D renderings using the 3D creator software supplied with the instrument. The resolution of the μCT images is 18.2 μm.

Histology

Tibias were removed and fixed in PLP fixative (2% paraformaldehyde containing 0.075 M lysine and 0.01 M sodium periodate) overnight at 4°C and processed histologically as described previously [16]. Proximal ends of each tibia were decalcified in EDTA glycerol solution for 5 to 7 days at 4°C. Decalcified tibias were dehydrated and embedded in paraffin, after which 5 μm sections were cut on a rotary microtome. The sections were stained with hematoxylin and eosin (H&E) or histochemically for total collagen (TCOL) or alkaline phosphatase activity (ALP), or tartrate-resistant acid phosphatase (TRAP) activity, or immunohistochemistry. Alternatively, undecalcified tibiae were embedded in LR White acrylic resin (London Resin Company, Ltd., London, UK), and 1 μm sections were cut on an ultramicrotome. These sections were observed under fluorescence microscopy.

Immunohistochemical staining

Immunohistochemical staining was carried out for proliferating cell nuclear antigen (PCNA), collagen type I (Col-I), and osteocalcin (OCN) using an avidin-biotin-peroxidase complex technique with an affinity-purified goat anti-rabbit PCNA antibody (Abcam, UK), an affinity-purified goat anti-mouse Col-I antibody (Santa Cruz, CA,

USA), and an affinity-purified goat anti-mouse OCN (Cell Signal, China). Briefly, dewaxed and rehydrated paraffin-embedded sections were incubated with methanol-hydrogen peroxide (1:10) to block endogenous peroxidase activity and then washed in Tris-buffered saline (pH 7.6). The slides were then incubated with the primary antibodies overnight at room temperature. After rinsing with Tris-buffered saline for 15 min, sections were incubated with biotinylated secondary antibody (Sigma, St. Louis, MO, USA). Sections were then washed and incubated with the Vectastain Elite ABC reagent (Vector Laboratories, Burlington, Canada) for 45 min. After washing, brown pigmentation was likewise produced using 3,3-diaminobenzidine (DAB). Finally, the stained sections were counterstained with H&E staining. Images were acquired with a Leica microscope (Leica DM4000B, Solms, Germany) equipped with Leica software.

Evaluation of apoptotic cells by TUNEL staining

The apoptotic cells from tibias were evaluated using terminal dexynucleotidyl transferase (TdT)-mediated dUTP nick end labelingthe (TUNEL) technique (20 mg/mL, Cat. no. 21627, Chemicon International, Temecula, CA, USA) [18]. To count the TUNEL-positive cells in the parotid glands tissue, a ocular micrometer compatible with an Olympus BX51 microscope was used.

Western blot analysis

Proteins were extracted from the femurs and quantitated by a kit (Bio-Rad, Mississauga, Ontario, Canada). Protein samples were fractionated by SDS-PAGE and transferred to nitrocellulose membranes. Western blot was carried out using antibodies against Caspase-3 (goat anti-rabbit, Cell Signal, China), γH2AX (goat anti-mouse, Santa Cruz, CA, USA), and β-actin (goat anti-rabbit, Santa Cruz Biotechnology, USA). Bands were visualized using enhanced chemiluminescence (ECL, Amersham) and quantitated by Scion Image Beta 4.02 (Scion Corporation, Bethesda, MD, USA).

Detection of ROS levels

Bone marrow cells from femur tissues were converted into single-cell suspensions containing 5×10^5 cells/mL. We used 2',7'-dichlorofluorescein diacetate (DCFH-DA, Sigma, USA) for detection of intracellular ROS. Fluorescence intensity is proportional to oxidant production. DCFH-DA was added to bone cell suspensions to yield final concentrations of 20 μmol/L. Then, cells were incubated at 37°C for 30 min in the dark, washed twice with 0.01 mol/L phosphate-buffered saline (PBS), and centrifuged at ×300 g for 5 min. ROS levels were measured by mean fluorescence intensity (MFI) of 10,000 cells using a flow cytometer (Becton, Dickinson and Co., USA). At the same time, immunofluorescence analysis for ROS levels of BMSC from femurs tissues was carried out as described previously.

Computer-assisted image analysis

After hematoxylin and eosin staining or histochemical or immunohistochemical staining of sections from both groups of 10 mice each, images of interesting fields were photographed with a SONY digital camera. Images of micrographs from single section were digitally recorded using a rectangular template, and recordings were processed and analyzed using Northern Eclipse image analysis software.

Statistical analysis

All analyses were carried out by SPSS software (version 20.0, SPSS Inc.). Data from image analysis were presented as mean ± standard error. Two-way ANOVA was used for statistical comparison and to make two-group comparisons. Qualitative data were described as percentages and analyzed using a chi-square test as indicated. All graphs were generated using GraphPad Software (version 5.0, USA). *p* values were two-sided, and $P<0.05$ was considered statistically significant.

Results

Effect of Bmi-1 on phenotype, body weight, percent survival and tibia length in mice

To investigate whether Bmi-1 could rescue a premature aging phenotype, we proceeded with analysis of phenotype (**Figure 1A**), body weight (**Figure 1C**), and percent survival (**Figure 1D**) in both groups of 7-week-old mice (10 WT mice, 10 BKO mice). Compared with WT mice, Bmi-1 knockout mice showed significant pre-

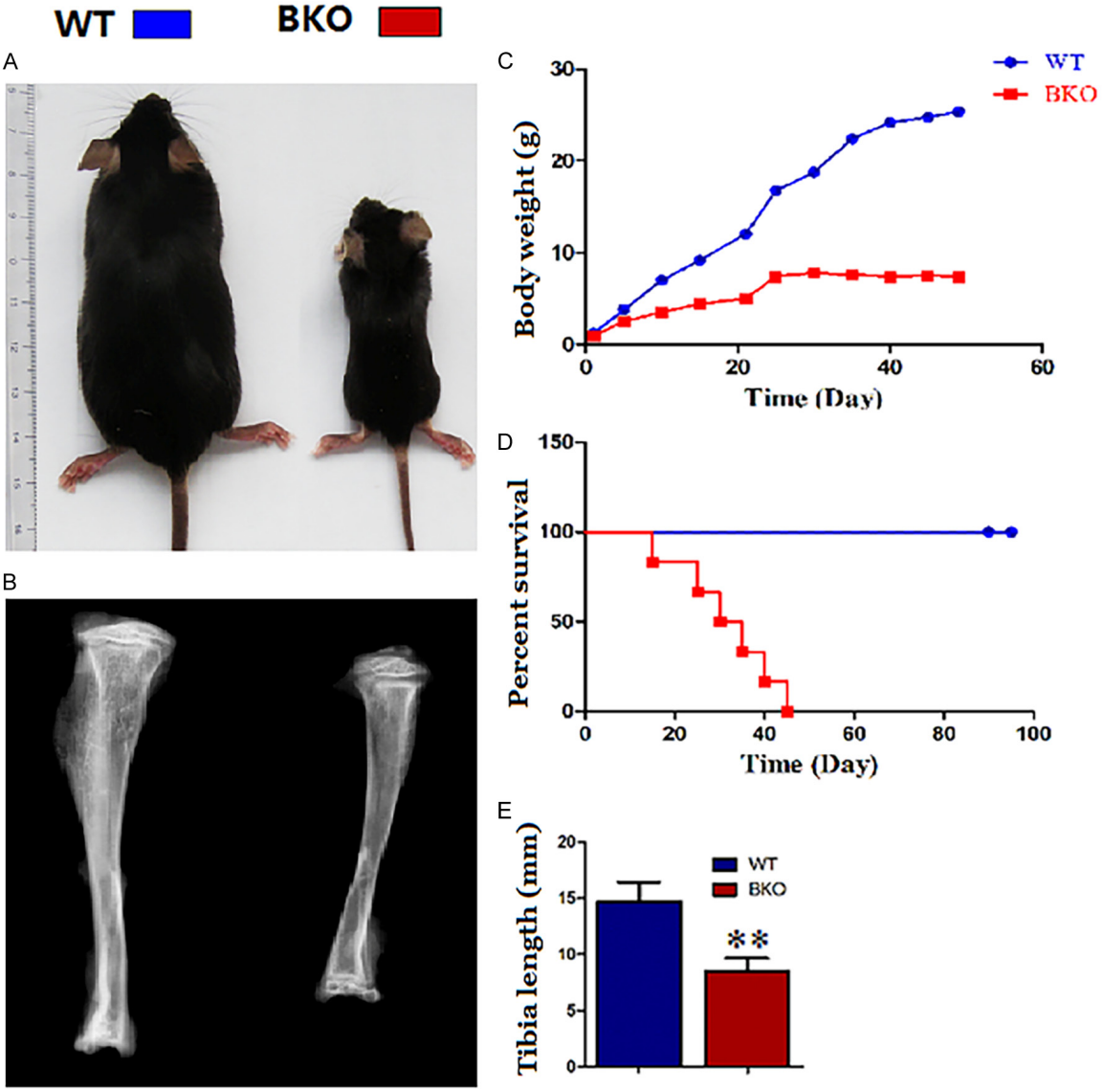

Figure 1. Role of PQQ in phenotype, body weight, percent survival and tibia length of mice. A. Effect of Bmi-1 on phenotype of mice. B. Radiographs of the tibiae of wild-type (WT), Bmi-1$^{-/-}$ mice (BKO). C. Effect of Bmi-1 on body weight of mice. D. Effect of Bmi-1 on percent survival of mice. E. Statistics of tibiae length.

mature aging phenotype, body weight loss and shorter percent survival. The results demonstrated that Bmi-1 could partly rescue premature aging phenotype, body weight, percent survival. To determine whether Bmi-1 could correct bone growth retardation in BKO mice, we analyzed and compared related parameters of bone growth in both groups of mice with X-ray photography (**Figure 1B**). These data showed that the size and length of the tibias (**Figure 1E**) were significantly increased in WT mice related to BKO mice.

Role of Bmi-1 in growth, proliferation and apoptosis in the tibia

To investigate whether Bmi-1 could promote proliferation and reduce apoptosis in the tibia, we comparatively analyzed related parameters of growth plate width (**Figure 2A**), PCNA IHC (**Figure 2C**) and TUNEL staining (**Figure 2E**). Our results showed that BKO mice had significantly decreased growth plate width of the tibia (**Figure 2B**), and PCNA positive cell percentage of cartilage (**Figure 2D**) compared with WT

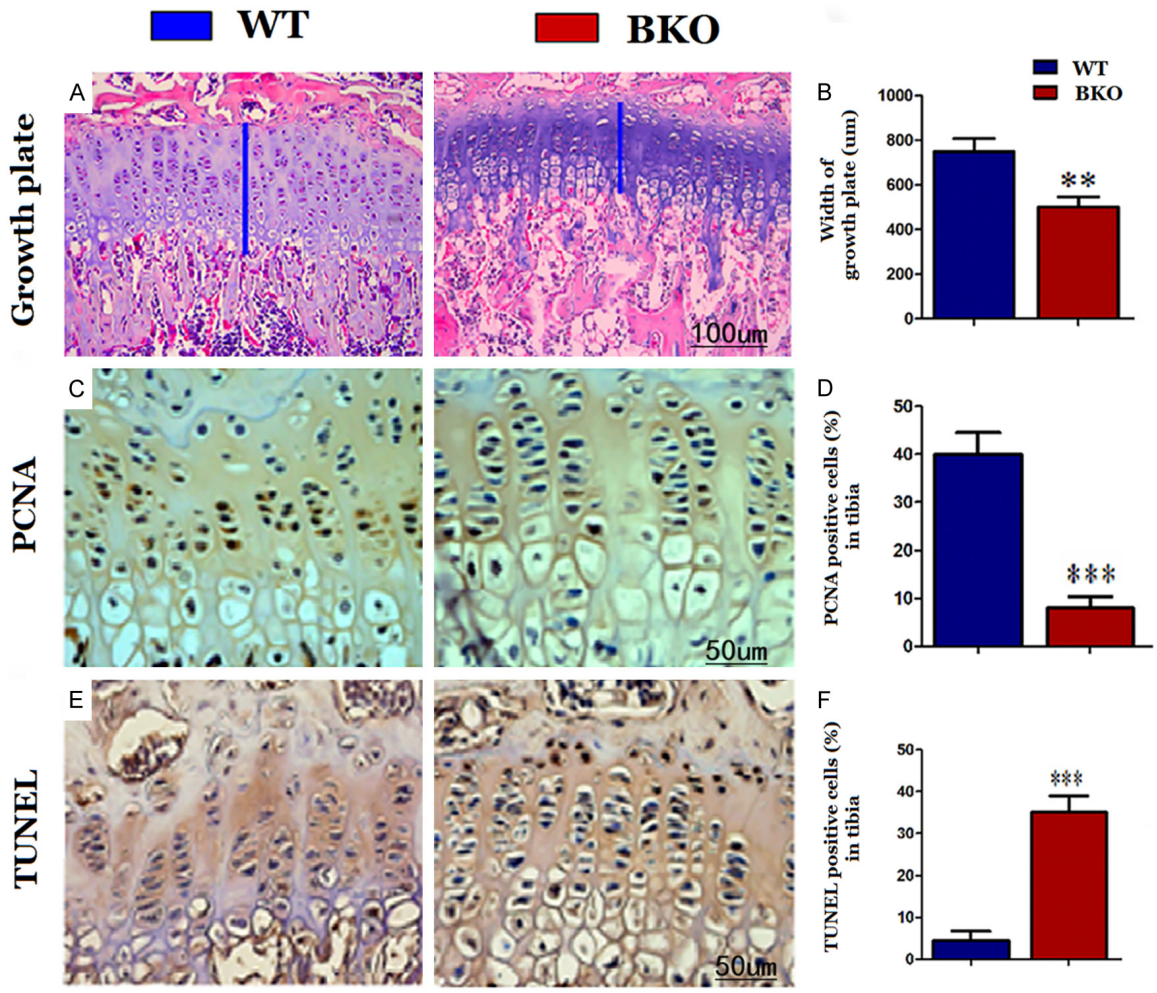

Figure 2. Role of Bmi-1 in growth, proliferation and apoptosis of tibiae. A. H&E staining of proximal tibial growth plate cartilage, the blue line represents growth plate cartilage (Original magnification ×200, scale bar: 100 μm). B. Statistics of tibial growth plate cartilage width. C. PCNA immunohistochemical staining micrograhps of proximal tibial growth plate cartilage (Original magnification ×400, scale bar: 50 μm). D. Statistics of PCNA positive cell percentage. E. TUNEL staining micrograhps of proximal tibial growth plate cartilage (Original magnification ×400, scale bar: 50 μm). F. Statistics of TUNEL positive cell percentage. Each value is the mean ± SEM of determinations in ten animals of the same groups. *, P<0.05; **, P<0.01; ***, P<0.001, compared with BKO mice.

mice. However, BKO mice had apparently increased percentage of TUNEL positive cells (**Figure 2F**) compared with WT mice. These data showed that Bmi-1 may promote cell proliferation and inhibit cell apoptosis to ameliorate bone growth retardation.

Role of Bmi-1 in trabecular bone volume of the tibia

To investigate whether Bmi-1 could improve the phenotype of bone senescence, two different phenotypes of tibia bones between 7-week-old WT mice and littermates BKO mice were analyzed by Micro-CT scanning (**Figure 3A**), H&E and TCOL staining (**Figure 3B**). Our data demonstrated that tibial trabecular bone volume and thickness of bone cortex were apparently decreased in BKO mice related to WT mice as shown in **Figure 3C**. Our results suggested that Bmi-1 could delay the phenotype of long bone senescence.

Role of Bmi-1 in osteoblast formation of tibiae

To determine the role of Bmi-1 in osteoblast formation of the tibia, we conducted experiments with H&E staining (**Figure 4A**), ALP staining (**Figure 4B**), Col-I (**Figure 4C**) and OCN (**Figure 4D**) IHC staining in the two different tibiae

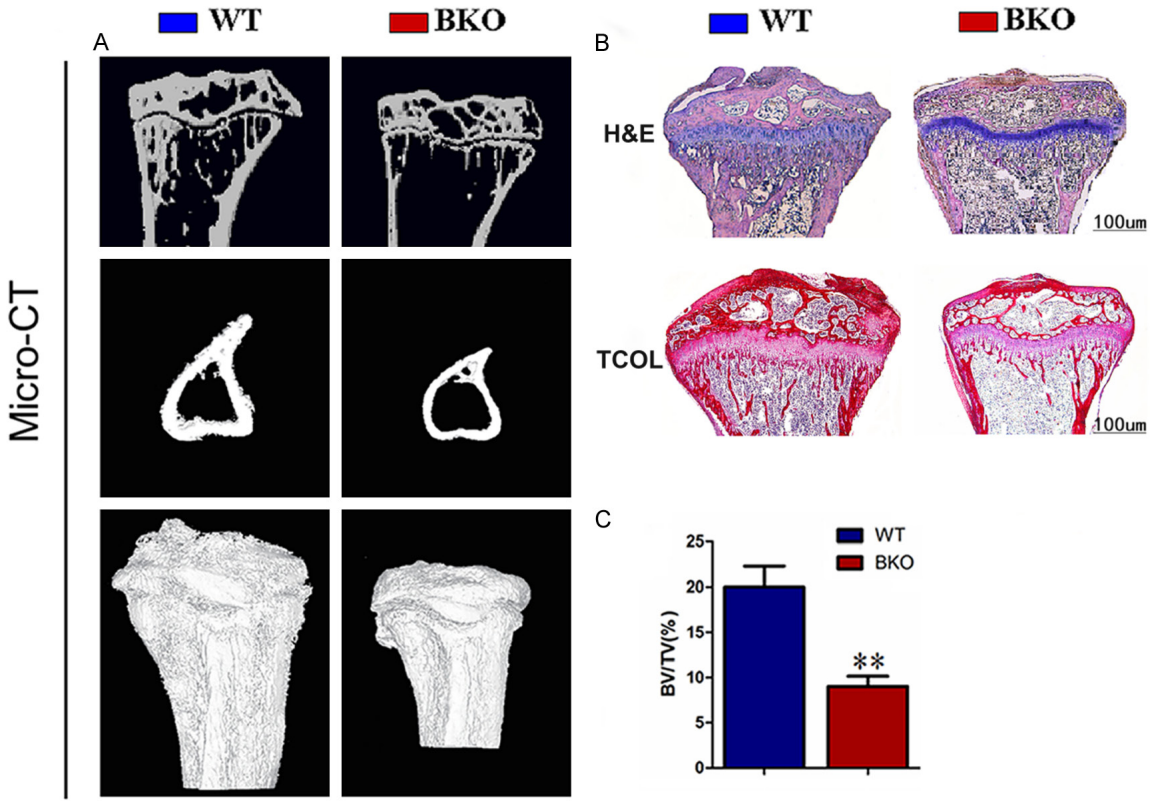

Figure 3. Role of Bmi-1 in trabecular bone volume of tibiae. A. 3-dimensional reconstructed longitudinal sections of micro-CT scanning images. B. Micrographs of paraffin sections of the tibiae stained with H&E and Sirius Red for total collagen (TCOL) from 7-week-old WT and BKO mice (Original magnification ×50, scale bar: 100 μm). C. Quantitation of trabecular bone volume relative to tissue volume (BV/TV, %) in metaphyseal regions. Each value is the mean ± SEM of determinations in six animals of the same groups. *, P<0.05; **, P<0.01; ***, P<0.001, compared with BKO mice.

groups. The results demonstrated that osteogenic cell (**Figure 4E**), osteoblast positive cell areas (**Figure 4F**), ALP (**Figure 4G**), Col-I (**Figure 4H**) and OCN (**Figure 4I**) positive areas were significantly increased in tibiae of WT mice compared with BKO mice. The results showed that Bmi-1 facilitated osteoblastic bone formation.

Role of Bmi-1 in osteoclast bone resorption, DNA damage and cell apoptosis of the tibia

To detect the role of Bmi-1 in osteoclast bone resorption, DNA damage and cell apoptosis of the tibia, we analyzed the number of osteoclasts in the tibia with TRAP staining (**Figure 5A**), γH2AX and Caspase-3 proteins with western blot (**Figure 5D**). Our data showed that the number of osteoclast positive cells (**Figure 5B**), and osteoclast positive cell areas (**Figure 5C**) were obviously increased in the tibia of BKO mice. Meanwhile, proteins levels of γH2AX and Caspase-3 were significantly increased in BKO mice related to WT mice (**Figure 5E**, **5F**). All the results suggested that Bmi-1 could attenuate osteoclast bone resorption abilities by reducing DNA damage and cell apoptosis.

Role of Bmi-1 in ROS levels of bone marrow mesenchymal stem cells (BMSC)

Previous studies suggested that the excess ROS and oxygen free radicals subsequently lead to the increase of DNA double strand breaks. To investigate whether Bmi-1 could reduce production of ROS and reduce DNA damage we conducted statistical analysis of ROS levels of the femur. Our results suggested that Bmi-1 decreased ROS levels of BMSC in femurs compared with BKO mice (**Figure 6A-C**). These data suggested that Bmi-1 could prevent an excess of ROS levels in BKO mice.

Discussion

Aging is associated with increased cellular senescence, which is hypothesized to drive the

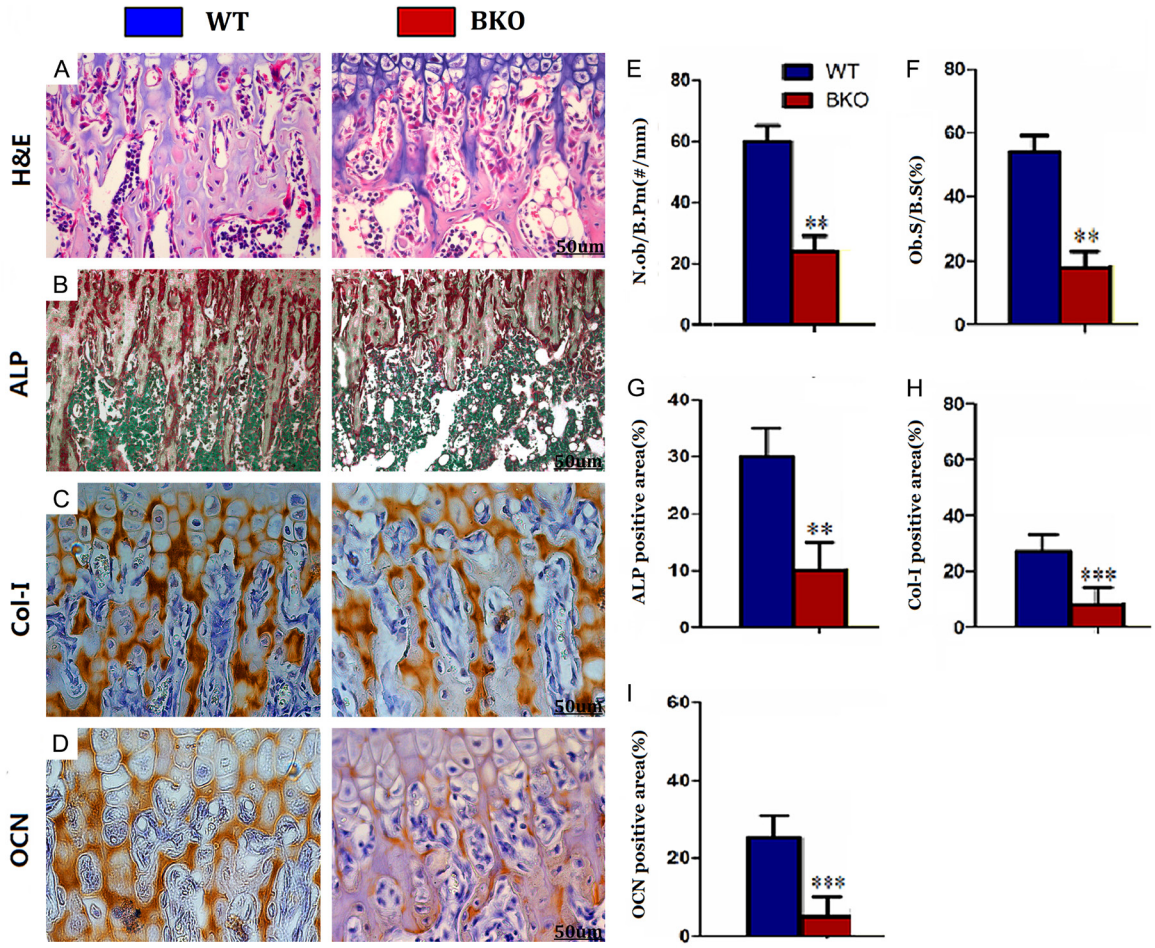

Figure 4. Role of Bmi-1 in osteoblast formation of tibiae. A. Micrographs of H&E staining of tibiae (Original magnification ×400, scale bar: 50 μm). B. Micrographs of ALP staining of the tibiae (Original magnification ×400, scale bar: 50 μm). C. Micrographs of Col-I immunohistochemical staining of tibiae (Original magnification ×400, scale bar: 50 μm). D. Micrographs of OCN immunohistochemical staining of tibiae (Original magnification ×400, scale bar: 50 μm). E. Number of positive osteoblasts of tibiae. F. Percentage of positive areas osteoblast of tibiae. G. ALP positive areas of tibiae. H. Col-I positive areas percentage of tibiae. I. OCN positive areas percentage of tibiae. Each value is the mean ± SEM of determinations in ten animals of the same groups. *, P<0.05; **, P<0.01; ***, P<0.001, compared with BKO mice. Number of positive osteoblasts (N.Ob/B.Pm, #/mm). Percent ratio of positive areas osteoblasts (Ob.S/B.S, %).

eventual development of multiple comorbidities. Here we investigate a role for senescent cells in age-related bone loss through multiple approaches. Aging bone related disease-osteoporosis is characterized by less bone mass and degradation of the microstructure of bone tissue, which leads to compromised bone strength and increased risk of fracture [2]. Bmi-1 can restore the balance of bone metabolism and limit bone loss in osteoporosis. It was well established that PQQ played an important therapeutic role in defective teeth and mandibles induced by Bmi-1 deficiency through increasing osteoblastic bone formation, decreasing osteoclast bone resorption, reducing ROS levels and retarding DNA damage [9]. It has been elucidated that the osteogenic mode of alveolar bone was intramembranous osteogenesis, meanwhile, long bone was cartilage osteogenesis. Our previous studies demonstrated that Bmi-1 could protect against oxidative stress in kidneys [19], skeletal muscle [20], brain [21] and hematopoietic stem cells [22]. The above data raises the hypothesis that Bmi-1 could play a key role in aging in long bones.

In our study, it was well established that Bmi-1 knockout mice resulted in growth retardation and premature aging phenotypes. Meanwhile, our results also demonstrated that the typical

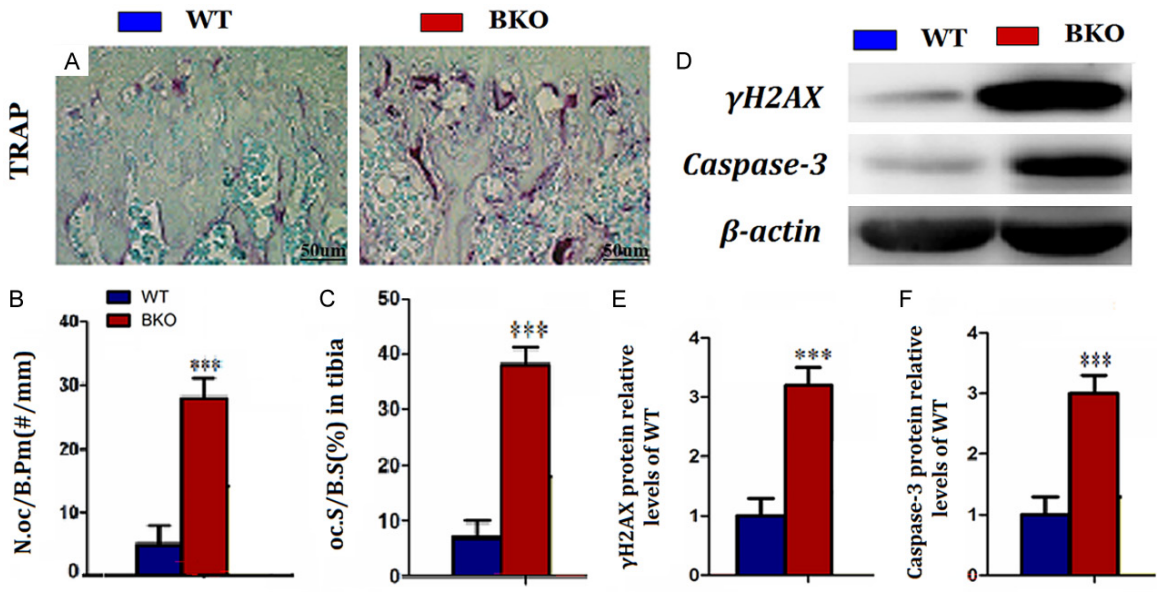

Figure 5. Role of PQQ in osteoclasts bone resorption, DNA damages and cell apoptosis of tibiae. (A) Micrographs of TRAP staining of tibiae (Original magnification ×400, scale bar: 50 μm). (B) Number of TRAP-positive osteoclasts of tibiae. (C) Surface of TRAP-positive osteoclasts of tibiae. (D) Representative tibiae western blot for expression of γH2AX and Caspase-3. β-actin was used as loading control for western blot in WT mice, BKO mice respectively. γH2AX (E) and Caspase-3 (F) proteins levels relative to β-actin protein levels were assessed by densitometric analysis and expressed relative to levels of WT mice. Each value is the mean ± SEM of determinations in ten animals of the same groups. *, P<0.05; **, P<0.01; ***, P<0.001, compared with BKO mice. Number of TRAP-positive osteoclasts (N.Oc/B.Pm, #/mm). Surface of TRAP-positive osteoclasts (Oc.S/B.S, %).

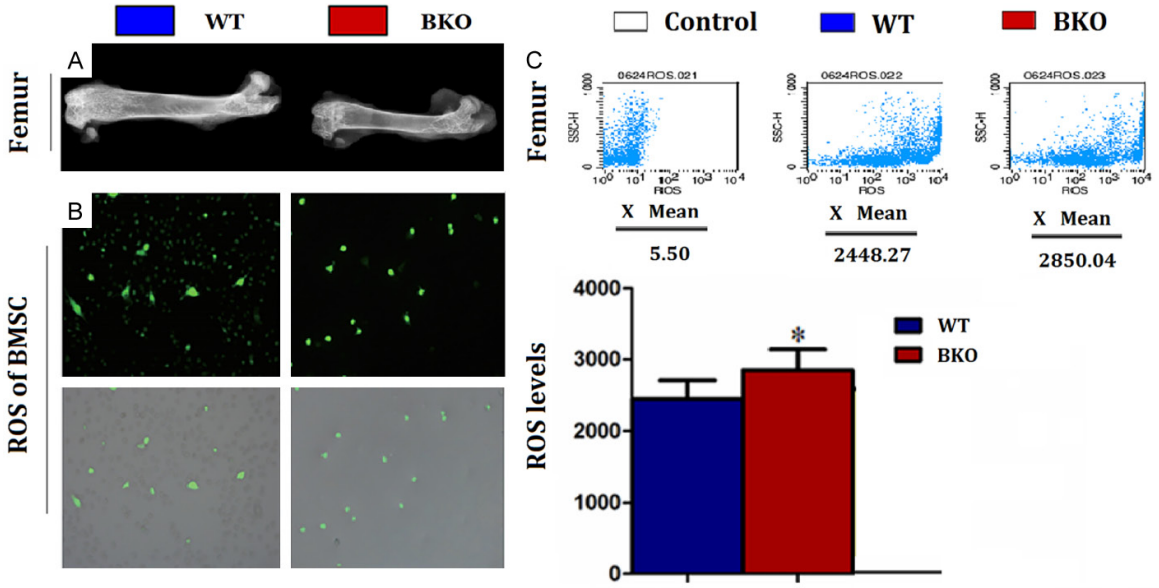

Figure 6. Role of Bmi-1 in ROS levels of BMSC of Femur. A. Radiographs of the tibiae of wild-type (WT), Bmi-1$^{-/-}$ mice (BKO); Flow cytometric analysis for ROS levels of femur in WT mice, BKO mice respectively. B. ROS levels of the femur. C. Immunofluorescence analysis for ROS levels of BMSC. Each value is the mean ± SEM of determinations in ten animals of the same groups. *, P<0.05; **, P<0.01; ***, P<0.001, compared with BKO mice.

aging and bone senescence phenotype in Bmi-1 knockout mice were partially corrected by the Bmi-1 gene through anti-aging, anti-apoptosis, proliferating, scavenging ROS and

reducing DNA damage. These findings indicated that Bmi-1 may play preventive and therapeutic roles in bone senescence and aging related degenerative diseases such as osteoporosis.

Previous study has shown that Bmi-1 gene deficient mice resulted in shortened life span and stunted growth [19]. Meanwhile, our study also investigated how BKO mice lead to shortened survival rates, low body weight and small overall size of the body. Our results revealed that the Bmi-1 gene could prolong survival, increase the overall body size by stimulating cell proliferation and inhibiting cell apoptosis. Thus, the Bmi-1 gene partially corrected the shortened life span and stunted growth in a model of systematic aging bone and aging related degenerative disease such as osteoporosis.

Osteoblastic and osteoclastic cells co-regulate bone metabolism, and they are the two kinds of cells involved in the development of bone senescence [23]. Osteoblasts are bone forming cells located near the surface of the bone that produces cytokines. Cytokines, are essential for osteoclast differentiation, function and survival [24, 25]. Osteoclasts are bone-absorbing polynucleated cells that bind tightly to the mineralized bone surface through integrins and secrete protons, proteases and superoxides through wrinkled boundaries to form absorption cavities [26-29]. Bone resorption is the formation of bone structure and bone remodeling caused by activated osteoclasts and the subsequent deposition of new substrates by osteoblasts [23]. The imbalance between bone formation and bone resorption is a key pathophysiological event in many metabolic bone diseases seen in adults, including bone aging and age-related degenerative diseases such as osteoporosis [30].

Our results suggested that Bmi-1 promoted long bone formation by inhibiting osteoclast bone resorption. Oxidative stress is a key pathogenic factor of age-related bone loss in mice [31-33], leading to changes such as increased osteoblast and osteocyte apoptosis, and decreased osteoblast number and bone formation rate via the Wnt/β-catenin signal pathway [32]. Previous studies suggested that oxidative stress inhibited osteoblast differentiation through extracellular signal-regulated kinases (ERKs) and ERK-dependent NF-κB signaling pathways [34-36]. Osteoblasts can produce antioxidants, such as glutathione peroxidase, to prevent excessive ROS production [37], as well as transforming growth factor β (TGF-β), which is involved in reducing bone resorption [38]. ROS also participated in bone resorption. Superoxides produced by osteoclasts directly promoted bone degradation, and oxidative stress increased the differentiation and function of osteoclasts [39-41]. Our data tested that excessive ROS levels in BKO mice were inhibited by Bmi-1. The above results showed that the Bmi-1 gene could reduce DNA damage through scavenging ROS of oxygen free radicals.

Our study well established that the Bmi-1 gene played an anti-osteoporosis role in osteoporosis of the long bone by regulating bone microenvironments such as stimulating osteoblast bone formation, decreasing osteoclast bone resorption, eliminating ROS levels and reducing DNA damage. However, this study has also certain limitations. Because the authors only showed that the Bmi-1 gene played an anti-aging role in bone in vivo, although not in vitro.

Conclusions

In conclusion, all the results of this study indicate that Bmi-1 plays an anti-aging role in bone in BKO mice via balancing oxidative stress. The study not only elucidates a novel mechanism of Bmi-1$^{-/-}$ inducing bone senescence, but also provides experimental and theoretical basis for using the Bmi-1 gene as a drug target to prevent Bmi-1$^{-/-}$ inducing long bone aging and age-related diseases such as osteoporosis.

Acknowledgements

The study was supported by a grant from the Scientific Research Project of Hunan Province Department of Education (Grant No. 22A0709).

Disclosure of conflict of interest

None.

Abbreviations

ALP, Alkaline phosphatase; Bmi-1, B cell-specific Moloney MLV insertion site-1; Bmi-1$^{+/-}$, Bmi-1 heterozygote; Bmi-1$^{-/-}$, Bmi-1 knock out homozygote; BKO, Bmi-1 knock out; BMSC, Bone marrow mesenchymal stem cells; Col-I, collagen

type I; DAB, 3,3-diaminobenzidine; DCFH-DA, 2',7'-dichlorofluo-rescein diacetate; ERKs, Extracellular signal-regulated kinases; H&E, hematoxylin and eosin; IHC, Immunohistochemical staining of tibiae; MFI, Mean fluorescence intensity; M-CSF, Macrophage colony-stimulating factor; Micro-CT, Micro-computed tomography; NAC, N-acetyl-L-cysteine; NF-κB, Receptor activator of nuclear factor κB; OCN, Osteocalcin; PBS, Phosphate-buffered saline; PCNA, Proliferating cell nuclear antigen; PcG, polycomb group; PQQ, Pyrroloquinoline quinone; γH2AX, Phosphorylate H2A histone, member X; RANKL, Ligand; ROS, Reactive oxygen species; TGF-β, Transforming growth factor β; TRAP, Tartrate-resistant acid phosphatase; TCOL, Total collagen; TUNEL, Terminal deoxynucleotidyl transferase (TdT)-mediated dUTP nick end labeling; WT, Wild type.

Address correspondence to: Dr. Yuanqing Huang, School of Stomatology, Hunan University of Medicine, No. 492 Jinxi South Road, Huaihua 418000, Hunan, China. Tel: +86-18942059592; E-mail: huang1977789@126.com

References

[1] Trivedi HD, Danford CJ, Goyes D and Bonder A. Osteoporosis in primary biliary cholangitis: prevalence, impact and management challenges. Clin Exp Gastroenterol 2020; 13: 17-24.

[2] Toy VE and Uslu MO. Evaluation of long-term dental implant success and marginal bone loss in postmenopausal women. Niger J Clin Pract 2020; 23: 147-153.

[3] Malod K, du Rand EE, Archer CR, Nicolson SW and Weldon CW. Oxidative damage is influenced by diet but unaffected by selection for early age of oviposition in the marula fly, ceratitis cosyra (diptera: tephritidae). Front Physiol 2022; 13: 794979.

[4] Wu J, Wang R, Kan X, Zhang J, Sun W, Goltzman D and Miao D. A Sonic Hedgehog-Gli-Bmi1 signaling pathway plays a critical role in p27 deficiency induced bone anabolism. Int J Biol Sci 2022; 18: 956-969.

[5] Tjempakasari A, Suroto H and Santoso D. Mesenchymal stem cell senescence and osteogenesis. Medicina (Kaunas) 2021; 58: 61.

[6] Yan L, Nielsen FH, Sundaram S and Cao J. Voluntary running of defined distances alters bone microstructure in C57BL/6 mice fed a high-fat diet. Appl Physiol Nutr Metab 2021; 46: 1337-1344.

[7] Zhang C, Meng Y and Han J. Emerging roles of mitochondrial functions and epigenetic changes in the modulation of stem cell fate. Cell Mol Life Sci 2024; 81: 26.

[8] Mohamad NV, Ima-Nirwana S and Chin KY. Are oxidative stress and inflammation mediators of bone loss due to estrogen deficiency? A review of current evidence. Endocr Metab Immune Disord Drug Targets 2020; 20: 1478-1487.

[9] Huang Y, Chen N and Miao D. Pyrroloquinoline quinone plays an important role in rescuing Bmi-1$^{-/-}$ mice induced developmental disorders of teeth and mandible--anti-oxidant effect of pyrroloquinoline quinone. Am J Transl Res 2018; 10: 40-53.

[10] Huang Y, Chen N and Miao D. Effect and mechanism of pyrroloquinoline quinone on anti-osteoporosis in Bmi-1 knockout mice-anti-oxidant effect of pyrroloquinoline quinone. Am J Transl Res 2017; 9: 4361-4374.

[11] Supruniuk E, Mikłosz A and Chabowski A. Pyrroloquinoline quinone modifies lipid profile, but not insulin sensitivity, of palmitic acid-treated L6 myotubes. Int J Mol Sci 2020; 21: 8382.

[12] Cheng Q, Chen J, Guo H, Lu JL, Zhou J, Guo XY, Shi Y, Zhang Y, Yu S, Zhang Q and Ding F. Pyrroloquinoline quinone promotes mitochondrial biogenesis in rotenone-induced Parkinson's disease model via AMPK activation. Acta Pharmacol Sin 2021; 42: 665-678.

[13] Ulla A, Uchida T, Miki Y, Sugiura K, Higashitani A, Kobayashi T, Ohno A, Nakao R, Hirasaka K, Sakakibara I and Nikawa T. Morin attenuates dexamethasone-mediated oxidative stress and atrophy in mouse C2C12 skeletal myotubes. Arch Biochem Biophys 2021; 704: 108873.

[14] Shi C, Yu Z, Wang Z, Ning R, Huang C, Gao Y and Wang F. Dietary supplementation with pyrroloquinoline quinone promotes growth, relieves weaning stress, and regulates metabolism of piglets compared with adding zinc oxide. Anim Nutr 2023; 15: 409-419.

[15] Ma K, Wu ZZ, Wang GL and Yang XP. Separation and purification of pyrroloquinoline quinone from Gluconobacter oxydans fermentation broth using supramolecular solvent complex extraction. Food Chem 2021; 361: 130067.

[16] Ji X, Chen H, Liu B, Zhuang H and Bu S. Chk2 deletion rescues Bmi1 deficiency-induced mandibular osteoporosis by blocking DNA damage response pathway. Am J Transl Res 2023; 15: 2220-2232.

[17] Pang Y, Qin M, Hu P, Ji K, Xiao R, Sun N, Pan X and Zhang X. Resveratrol protects retinal ganglion cells against ischemia induced damage by increasing Opa1 expression. Int J Mol Med 2020; 46: 1707-1720.

[18] Yan R, Cui F, Dong L, Liu Y, Chen X and Fan R. Repression of PCGF1 decreases the proliferation of glioblastoma cells in association with inactivation of c-Myc signaling pathway. Onco Targets Ther 2020; 13: 253-261.
[19] Chen H, Zhou J, Chen H, Liang J, Xie C, Gu X, Wang R, Mao Z, Zhang Y, Li Q, Zuo G, Miao D and Jin J. Bmi-1-RING1B prevents GATA4-dependent senescence-associated pathological cardiac hypertrophy by promoting autophagic degradation of GATA4. Clin Transl Med 2022; 12: e574.
[20] Lian D, Chen MM, Wu H, Deng S and Hu X. The role of oxidative stress in skeletal muscle myogenesis and muscle disease. Antioxidants (Basel) 2022; 11: 755.
[21] Whittaker DS, Akhmetova L, Carlin D, Romero H, Welsh DK, Colwell CS and Desplats P. Circadian modulation by time-restricted feeding rescues brain pathology and improves memory in mouse models of Alzheimer's disease. Cell Metab 2023; 35: 1704-1721, e6.
[22] Wang R, Xue X, Wang Y, Zhao H, Zhang Y, Wang H and Miao D. BMI1 deficiency results in female infertility by activating p16/p19 signaling and increasing oxidative stress. Int J Biol Sci 2019; 15: 870-881.
[23] Zhang L, Luo Q, Shu Y, Zeng Z, Huang B, Feng Y, Zhang B, Wang X, Lei Y, Ye Z, Zhao L, Cao D, Yang L, Chen X, Liu B, Wagstaff W, Reid RR, Luu HH, Haydon RC, Lee MJ, Wolf JM, Fu Z, He TC and Kang Q. Transcriptomic landscape regulated by the 14 types of bone morphogenetic proteins (BMPs) in lineage commitment and differentiation of mesenchymal stem cells (MSCs). Genes Dis 2019; 6: 258-275.
[24] Zhao Y, Wang HL, Li TT, Yang F and Tzeng CM. Baicalin ameliorates dexamethasone-induced osteoporosis by regulation of the RANK/RANKL/OPG signaling pathway. Drug Des Devel Ther 2020; 14: 195-206.
[25] Chen X, Wang Z, Duan N, Zhu G, Schwarz EM and Xie C. Osteoblast-osteoclast interactions. Connect Tissue Res 2018; 59: 99-107.
[26] Li S, Li Q, Zhu Y and Hu W. GDF15 induced by compressive force contributes to osteoclast differentiation in human periodontal ligament cells. Exp Cell Res 2020; 387: 111745.
[27] Takayanagi H. RANKL as the master regulator of osteoclast differentiation. J Bone Miner Metab 2021; 39: 13-18.
[28] Ekeuku SO, Pang KL and Chin KY. Effects of caffeic acid and its derivatives on bone: a systematic review. Drug Des Devel Ther 2021; 15: 259-275.
[29] Liu X, Diao L, Zhang Y, Yang X, Zhou J, Mao Y, Shi X, Zhao F and Liu M. Piperlongumine inhibits titanium particles-induced osteolysis, osteoclast formation, and RANKL-induced signaling pathways. Int J Mol Sci 2022; 23: 2868.
[30] Xu Z, Zhang X, Wang Y, Hao X, Liu M, Sun J and Zhao Z. Comparison of bone-setting robots and conventional reduction in the treatment of intertrochanteric fracture: a retrospective study. Orthop Surg 2024; 16: 312-319.
[31] Marcucci G, Domazetovic V, Nediani C, Ruzzolini J, Favre C and Brandi ML. Oxidative stress and natural antioxidants in osteoporosis: novel preventive and therapeutic approaches. Antioxidants (Basel) 2023; 12: 373.
[32] Solgi S, Zayeri F and Abbasi B. The reverse association of dietary antioxidant index with osteoporosis in postmenopausal iranian women: a case-control study. J Res Med Sci 2023; 28: 64.
[33] Ma Y, Wang S, Wang H, Chen X, Shuai Y, Wang H, Mao Y and He F. Mesenchymal stem cells and dental implant osseointegration during aging: from mechanisms to therapy. Stem Cell Res Ther 2023; 14: 382.
[34] Qin R, Sun J, Wu J and Chen L. Pyrroloquinoline quinone prevents knee osteoarthritis by inhibiting oxidative stress and chondrocyte senescence. Am J Transl Res 2019; 11: 1460-1472.
[35] Choi EM, Suh KS, Jung WW, Yun S, Park SY, Chin SO, Rhee SY and Chon S. Catalpol protects against 2,3,7,8-tetrachlorodibenzo-p-dioxin-induced cytotoxicity in osteoblastic MC3T3-E1 cells. J Appl Toxicol 2019; 39: 1710-1719.
[36] Salman S, Guermonprez C, Peno-Mazzarino L, Lati E, Rousseaud A, Declercq L and Kerdine-Römer S. Photobiomodulation controls keratinocytes inflammatory response through Nrf2 and reduces langerhans cells activation. Antioxidants (Basel) 2023; 12: 766.
[37] Qian F, Misra S and Prabhu KS. Selenium and selenoproteins in prostanoid metabolism and immunity. Crit Rev Biochem Mol Biol 2019; 54: 484-516.
[38] Mao D, Pan X, Rui Y and Li F. Matrine attenuates heterotopic ossification by suppressing TGF-β induced mesenchymal stromal cell migration and osteogenic differentiation. Biomed Pharmacother 2020; 127: 110152.
[39] Angireddy R, Kazmi HR, Srinivasan S, Sun L, Iqbal J, Fuchs SY, Guha M, Kijima T, Yuen T, Zaidi M and Avadhani NG. Cytochrome c oxidase dysfunction enhances phagocytic function and osteoclast formation in macrophages. FASEB J 2019; 33: 9167-9181.
[40] Padrón-Monedero A. A pathological convergence theory for non-communicable diseases. Aging Med (Milton) 2023; 6: 328-337.
[41] Klimova N, Fearnow A, Long A and Kristian T. NAD+ precursor modulates post-ischemic mitochondrial fragmentation and reactive oxygen species generation via SIRT3 dependent mechanisms. Exp Neurol 2020; 325: 113144.